International Journal for Parasitology 40 (2010) 695–703

Contents lists available at ScienceDirect

International Journal for Parasitology

journal homepage: www.elsevier.com/locate/ijpara

Metabolic alterations in the hamster co-infected with *Schistosoma japonicum* and *Necator americanus*

Jun-Fang Wu [a,b], Elaine Holmes [c], Jian Xue [d], Shu-Hua Xiao [d], Burton H. Singer [e], Hui-Ru Tang [a], Jürg Utzinger [f], Yu-Lan Wang [a,*]

[a] *State Key Laboratory of Magnetic Resonance and Atomic and Molecular Physics, Wuhan Center for Magnetic Resonance, Wuhan Institute of Physics and Mathematics, Chinese Academy of Sciences, Wuhan 430071, People's Republic of China*
[b] *Graduate School of Chinese Academy of Sciences, Beijing 100049, People's Republic of China*
[c] *Biomolecular Medicine, Department of Surgery and Cancer, Faculty of Medicine, Imperial College London, Sir Alexander Fleming Building, South Kensington, London SW7 2AZ, UK*
[d] *National Institute of Parasitic Diseases, Chinese Center for Disease Control and Prevention, Shanghai 200025, People's Republic of China*
[e] *Office of Population Research, Princeton University, 245 Wallace Hall, Princeton, NJ 08544, USA*
[f] *Department of Public Health and Epidemiology, Swiss Tropical Institute, P.O. Box, CH-4002 Basel, Switzerland*

ARTICLE INFO

Article history:
Received 23 September 2009
Received in revised form 3 November 2009
Accepted 4 November 2009

Keywords:
Co-infection
Hamster
Metabonomics
Necator americanus
NMR spectroscopy
Schistosoma japonicum

ABSTRACT

Co-infection with hookworm and schistosomes is a common phenomenon in sub-Saharan Africa, as well as in parts of South America and southeast Asia. As a first step towards understanding the metabolic response of a hookworm-schistosome co-infection in humans, we investigated the metabolic consequences of co-infection in an animal model, using a nuclear magnetic resonance (NMR)-based metabolic profiling technique, combined with multivariate statistical analysis. Urine and serum samples were obtained from hamsters experimentally infected with 250 *Necator americanus* infective L_3 and 100 *Schistosoma japonicum* cercariae simultaneously. In the co-infection model, similar worm burdens were observed as reported for single infection models, whereas metabolic profiles of co-infection represented a combination of the altered metabolite profiles induced by single infections with these two parasites. Consistent differences in metabolic profiles between the co-infected and non-infected control hamsters were observed from 4 weeks p.i. onwards. The predominant metabolic alterations in co-infected hamsters consisted of depletion of amino acids, tricarboxylic acid cycle intermediates (e.g. citrate and succinate) and glucose. Moreover, alterations of a series of gut microbial-related metabolites, such as decreased levels of hippurate, 3-hydroxyphenylpropionic acid, 4-hydroxyphenylpropionic acid and trimethylamine-*N*-oxide, and increased concentrations of 4-cresol glucuronide and phenylacetylglycine were associated with co-infection. Our results provide a first step towards understanding the metabolic response of an animal host to multiple parasitic infections.

1. Introduction

Polyparasitism is the co-occurrence of two or more parasite species in the same organism. This phenomenon is common in regions where different parasites co-exist at high frequencies (Petney and Andrews, 1998). For example, a considerable proportion of people have been found to be concurrently infected with multiple parasite species in rural parts of China (Yu et al., 1994; Steinmann et al., 2008) and across Africa (Raso et al., 2004; McKenzie, 2005). Hookworm and schistosomiasis are among the most frequent co-existing parasitic diseases, mainly in sub-Saharan Africa, as well as in parts of South America and southeast Asia. A significant positive association between *Schistosoma mansoni* and hookworm was noted in villages in western Côte d'Ivoire and Uganda (Keiser et al., 2002; Raso et al., 2004; Fleming et al., 2006), probably explained by shared transmission routes (Petney and Andrews, 1998). The co-infection rate of these two parasites has been reported to reach approximately 20% in schoolchildren in western Côte d'Ivoire (Raso et al., 2006) and 41% in a region of southeast Brazil (Pullan et al., 2008).

A concurrent infection with hookworms and schistosomes has been shown to result in a higher rate of anaemia compared with single infections (Brito et al., 2006). The different types of co-existing parasites can result in synergistic or antagonistic interactions in terms of worm burden within a mammalian host. Positive or negative associations among the pathogenic effects subsequently result in either exacerbated or suppressed clinical manifestations (Keusch and Migasena, 1982; Behnke et al., 2001). For example, a host infected with *S. mansoni* had the ability to expel a subsequent *Trichuris muris* infection (Curry et al., 1995), and to inhibit the viability of *Strongyloides venezuelensis* worms (Yoshida et al., 1999).

* Corresponding author. Tel.: +86 27 8719 7143; fax: +86 27 8719 9291.
E-mail address: yulan.wang@wipm.ac.cn (Y.-L. Wang).

0020-7519/$36.00 © 2009 Australian Society for Parasitology Inc. Published by Elsevier Ltd. All rights reserved.
doi:10.1016/j.ijpara.2009.11.003

Mice co-infected with *Litomosoides sigmodontis* and *Leishmania major* showed delayed development of leishmanial lesions, suggesting that there can be beneficial effects with co-infection (Lamb et al., 2005). Studies have shown that the immunological interactions between the parasites and co-infected hosts mainly accounted for the synergistic or antagonistic reaction observed (Naus et al., 2003; Fenton et al., 2008). For example, mice previously exposed to radiation-attenuated *S. mansoni* cercariae showed an increased antibody response against somatic antigens from the hookworm *Necator americanus*, and proved cross-reactive against poly-parasitic antigens (Timothy et al., 1992). On the contrary, patients infected with *S. mansoni* expressed lower humoral and cellular responses to hookworm than patients from areas non-endemic for *S. mansoni* (Correa-Oliveira et al., 2002). Given that the majority of investigations on co-infections are based on immunological studies, the metabolic consequences of co-infection remain to be elucidated. Understanding these metabolic consequences is important for clarifying the underlying molecular mechanisms of co-infection and could subsequently influence current strategies for deworming programmes. Although parasitic infections with multiple species are common in many parts of the world, it is not known how the treatment for one parasite influences the severity of the infection with other parasites.

The combination of ^{1}H nuclear magnetic resonance (NMR) spectroscopy of biofluids (e.g. plasma, serum and urine) or tissues with multivariate statistical analysis has demonstrated potential for identifying candidate biomarkers and deepening our understanding of mechanisms in clinical human diseases (Brindle et al., 2002; Sreekumar et al., 2009) and parasitic infections in rodent models (Li et al., 2008; Saric et al., 2008; Wang et al., 2008). To date, systematic ^{1}H NMR metabolic fingerprints have been applied to investigate the metabolic consequences of single infections with four parasitic worms, *S. mansoni* (Wang et al., 2004; Li et al., 2009), *Schistosoma japonicum* (Wang et al., 2006), *Echinostoma caproni* (Saric et al., 2008, 2009) and *N. americanus* (Wang et al., 2009), and two protozoa, *Plasmodium berghei* (Li et al., 2008) and *Trypanosoma brucei brucei* (Wang et al., 2008), in rodent models. In addition, a capillary electrophoresis technique has been employed to explore the metabolic response of a mouse to *S. mansoni* infection, providing complementary metabolic information to NMR spectroscopic profiling (Garcia-Perez et al., 2008).

As a first step towards understanding the mechanisms of poly-parasitism in humans, we investigated the dynamic metabolic effect of a *N. americanus–S. japonicum* co-infection in a hamster model with a view to elucidate metabolic interactions between these two parasites in the same host. In addition, we compared the similarities and differences between the metabolic consequences of a single infection and co-infection.

2. Materials and methods

2.1. Parasites, host and infection

The animal experiment was carried out at the National Institute of Parasitic Diseases, Chinese Center for Disease Control and Prevention (Shanghai, China), adhering to guidelines of the Chinese Academy of Sciences. Twenty male golden hamsters (*Mesocricetus auratus*), aged 6–7 weeks, were purchased from the Shanghai Animal Center, Chinese Academy of Sciences, and were housed in groups of five in plastic cages with free access to water and a rodent diet. After 1 week of acclimatisation, half of the hamsters (n = 10) were each co-infected with 250 infective L_3 of *N. americanus* and 100 *S. japonicum* cercariae via shaved abdominal skin and via s.c. injection, respectively (Xue et al., 2003). The remaining 10 hamsters were subjected to the same procedures without infection. The *N. americanus* eggs, obtained from hamsters fully adapted to this parasite through more than 100 generations (Xue et al., 2003), were cultivated to generate L_3, and *S. japonicum* cercariae were obtained from infected *Oncomelania hupensis* (Anhui isolate) after exposure to artificial light.

2.2. Sample collection and assessment of infection level

Blood serum and urine samples were collected at seven time points, i.e. 1 day before infection, day 1 p.i. and then at weekly intervals until week 5 p.i. Sample collection was carried out between 08:00 and 11:00 h in order to minimise potential metabolic variation due to the hamsters' diurnal cycle. Urine samples were collected by placing the hamsters individually in metabolic cages until approximately 0.4 ml of urine was produced. If less than 0.4 ml of urine was produced, the hamsters were administered 2 ml of tap water orally once every 30 min, two or three times, until a sufficiently large volume of urine was obtained. Urine samples were transferred into Eppendorf tubes and stored in a freezer at −80 °C. Blood samples (50–60 μl) were drawn from the retro-orbital plexus of each hamster via a capillary tube and transferred into 0.5 ml Eppendorf tubes. After centrifugation at 3,000*g* for 10 min, the serum (25–30 μl) was transferred into 0.5 ml Eppendorf tubes and kept at −80 °C for subsequent ^{1}H NMR analyses. Both infected and non-infected hamsters were sacrificed on day 37 p.i. Adult schistosomes were recovered from the portal vein and the mesenteric veins by perfusion via the heart with saline solution containing heparin. The worms were then sexed and counted to assess the infection level. Adult *N. americanus* were recovered from the small intestinal mucosa and the lumen of the hamsters. Two hamsters from the infected group died at weeks 2 and week 4 p.i., respectively, and hence were excluded from the analyses.

2.3. Preparation of samples and acquisition of ^{1}H NMR spectral data

The serum samples were prepared by mixing 30 μl of serum and 30 μl of PBS solution made up with 95% D_2O. The final concentration of PBS was 30 mM after adjusting for minor pH variations. After vortexing and centrifugation at 10,000*g*, at a temperature of 4 °C, the mixed liquid was transferred into 1.7-mm diameter micro NMR tubes (CortecNet, Paris, France) using a microsyringe (Hamilton, USA). The urine samples were prepared by adding D_2O to make a final volume of 500 μl. The liquid was mixed with 50 μl Na^+/K^+ buffer (K_2HPO_4/NaH_2PO_4, 1.5 M, pH 7.4), containing 0.01% sodium 3-trimethylsilyl (2,2,3,3-^{2}H4) propionate (TSP) for chemical shift reference purposes (Xiao et al., 2009). After vortexing and centrifugation at 10,000*g*, at 4 °C, 500 μl of the supernatant was transferred into 5-mm outer diameter NMR tubes (Norell, ST500-7, USA).

The ^{1}H NMR spectra of sera were recorded with a broad band inverse detection probe on a Bruker AVII 500 NMR spectrometer, operating at 500.13 MHz for proton frequency (Bruker, Biospin, Germany). The ^{1}H NMR spectra of urine were acquired with a cryogenic probe on a Bruker AVIII 600.13 MHz NMR spectrometer. A standard one-dimensional (1D) NMR experiment with water pre-saturation was performed for both urine and sera samples with pulse sequence (recycle delay (RD)-90°-t_1-90°-t_m-90°-acquisition), and an additional spin-relaxation edited NMR experiment was performed for sera with Carr–Purcell–Meiboom–Gill (CPMG) pulse sequence (RD-90°-(τ-180°-τ)$_n$-acquisition). The samples were maintained at an ambient temperature (25 °C) and the 90° pulse length was adjusted to ~10 μs. For the standard 1D NMR experiment, a RD of 2 s, a mixing time (t_m) of 100 ms and t_1 of 4 μs were used. The water peak was suppressed during the RD and t_m. For the CPMG experiment, a fixed total spin–spin relaxation delay of 70 ms ($2n\tau$) was applied to attenuate peaks arising from macromolecules in serum samples. A total of 256 and 32 scans

for serum and urine spectra, respectively, were recorded into 32*k* data points with a spectral width of 20 ppm. For serum resonance assignment purposes 2D NMR experiments, ^{1}H–^{1}H correlation spectroscopy (COSY) and total correlation spectroscopy (TOCSY) were performed with a total of 256 increments and 80 scans accumulated into 2*k* data points with a spectral width of 10 ppm for each dimension. For urine, 160 scans per increment and 64 increments were collected into 2*k* data points with a spectral width of 10.5 ppm by using MLEV-17 as a spin-lock scheme, with the mixing time of 80 ms. Moreover, heteronuclear multiple bond correlation spectroscopy (HMBC) and J-resolved spectroscopy were acquired on randomly selected urine samples. In HMBC, the spectral width was 10.5 ppm in the ^{1}H dimension and 220 ppm in the ^{13}C dimension, and 100 transients were collected into 2*k* data points for each of 320 increments. The data were zero-filled to 2*k* in both dimensions.

2.4. Data processing of NMR spectral data and multivariate pattern recognition

An exponential line broadening function of 0.5 Hz was applied to free induction decays (FIDs) prior to Fourier transformation. All ^{1}H NMR spectra were manually corrected for phase and baseline distortion (Bruker Biospin, Germany). Serum spectra were calibrated to an anomeric proton signal from α-glucose, at δ 5.23. Urine spectra were calibrated to TSP resonance at δ 0.0. The processed NMR spectra were data-reduced using the AMIX package (Bruker Biospin, Germany). The spectral regions δ 0.5–8.0 of serum were segmented into spectral regions of 0.004 ppm whereas the δ 0.5–9.5 regions of urine spectra were segmented into discrete regions of 0.002 ppm. Spectral regions δ 4.5–5.1 and δ 4.55–6.32 for serum and urine, respectively, were removed in order to eliminate variations caused by imperfect water suppression and/or proton exchange processes between the water and urea resonances. Additional resonances at δ 3.65 and δ 1.18 from sera spectra were removed due to contamination of the samples with ethanol introduced by swabbing during sample collection.

Normalisation of each spectrum to the total spectral intensity was carried out on the data prior to importing data into SIMCA-P^{+} software (Umetrics AB, Umea, Sweden) for pattern recognition analysis. In the first instance, principal component analysis (PCA) was performed using mean-centred NMR data to detect the general trends and outliers. Subsequently, a supervised multivariate data analysis tool, orthogonal projection to latent structure discriminant analysis (O-PLS-DA), was applied to the analysis of ^{1}H NMR spectral data, scaled to unit variance (Trygg and Wold, 2002; Vandenberg et al., 2006). The interpretation of the model was facilitated by back-scaled transformation of the loadings (Cloarec et al., 2005), with incorporated colour-coded correlation co-efficients of the metabolites responsible for the differentiation. The colour plot was obtained using version 7.1 of MATLAB (The Mathworks Inc., Natwick, USA) environment using an in-house developed script. In effect, each back-scale transformed loading is plotted as a function of the respective chemical shift with a colour code indicating the weights of the discriminatory variables. A hot colour (i.e. red) corresponds to the metabolite being highly significant (positive/negative) in discriminating between classes, while a cool colour (i.e. blue) corresponds to no significance. To check the model validity and avoid over-fitting of the PLS model, a sevenfold cross-validation method was used (repeatedly leaving out one-seventh of the samples and predicting them back into the model) and the cross-validation parameter Q^2 was calculated (Trygg et al., 2007). An additional cross-validation tool, a permutation test, was performed for each model by randomizing the order of *Y* variables for a specified number of times (permutation number = 200). The R^2 in the permutated plot described how well the data fit the derived model, whereas Q^2 describes the predictive ability of the derived model and provides a measure of the model quality. If higher Q^2s were obtained from permutation models than from the true model, then the model was deemed to lack predictive ability (Slupsky et al., 2007; Westerhuis et al., 2008).

2.5. Statistical analyses

The infection rate was analysed using SPSS 13.0 software and expressed as mean ± SD with the significance probability of 95% ($P < 0.05$). Statistical analysis of bivariate association between *N. americanus* and *S. japonicum* worm burden was carried out using Spearman's rank correlation co-efficient.

3. Results

3.1. Worm burden

Between 16 and 92 *S. japonicum* worms (mean = 53, SD = 26.5) and between eight and 36 hookworms (mean = 23, SD = 10.8) were obtained from the co-infected hamsters upon dissection. The individual worm burden of each hamster is listed in Table 1. The analysis revealed no statistically significant correlation between the worm burdens for the two parasite species ($P = 0.456$). Moreover, compared with the average infection rates for a single infection (*S. japonicum* or *N. americanus*) of hamsters at 5 weeks p.i. (by one sample *t*-test analysis), there were no statistically significant differences between the animals with a single infection and those with co-infection (Xue et al., 2003; Wang et al., 2006).

3.2. ^{1}H NMR spectra of urine and serum

Examples of typical ^{1}H NMR spectra of urine and ^{1}H CPMG NMR spectra of sera obtained from a hamster at three different time points, pre-infection and weeks 2 and 4 p.i., are shown in Figs. 1 and 2. Endogenous metabolites were assigned based on previously published work (Nicholson et al., 1995; Fan, 1996; Bollard et al., 2005), and confirmed with 2D TOCSY, COSY and HMBC spectra (data not shown). The metabolites identified in the ^{1}H NMR spectra of urine included a range of aliphatic organic acids (such as citrate, succinate, D-3-hydroxybutyrate (D-3-HB), butyrate, formate and acetate), aromatic metabolites (such as 4-ethylphenol, hippurate, 4-cresol glucuronide, phenylacetylglycine (PAG), 4-hydroxyphenylpropionic acid (4-HPPA) and 3-hydroxyphenylpropionic acid (3-HPPA)), and a range of amines (such as dimethylamine (DMA), dimethylglycine (DMG) and trimethylamine-*N*-oxide (TMAO)).

Metabolites found in sera of hamsters were mostly amino acids, carbohydrate metabolism-related metabolites including pyruvate, citrate, lipid-related metabolites, D-3-HB, acetoacetate, *scyllo*-inositol and membrane-related metabolites, such as choline, phosphorylcholine and glyceryl phosphorylcholine (GPC). It is clear from the visual inspection of the NMR spectra that the levels of D-3-HB were elevated in the sera of infected hamsters. Multivariate data analyses were subsequently performed to generate an overall metabolic response of hamsters to the *N. americanus*–*S. japonicum* co-infection (Trygg and Wold, 2002).

3.3. Metabolic profiling via ^{1}H NMR spectroscopy of urine

First, PCA between urine spectra obtained from *N. americanus* and *S. japonicum* co-infected hamsters and non-infected control hamsters at matched time points was performed to give an overview of the dataset. The PCA score plots showed that separation between co-infected and non-infected control hamsters was evident from week 3 p.i. onwards (data not shown). Pair-wise com-

Table 1
Worm burden in hamsters co-infected with 100 *Schistosoma japonicum* cercariae and 250 *Necator americanus* infective L_3 at 37 days p.i.

Hamster[a]	Schistosome				Hookworm			
	Female	Male	Total	Recovery rate (%)	Female	Male	Total	Recovery rate (%)
1	11	12	23	23	3	5	8	3.2
2	39	41	80	80	4	5	9	3.6
3	16	23	39	39	17	13	30	12
4	20	33	53	53	12	16	28	11.2
6	23	34	57	57	14	22	36	14.4
8	42	50	92	92	5	11	16	6.4
9	7	9	16	16	9	24	33	13.2
10	28	39	67	67	10	14	24	9.6

[a] Hamsters Nos. 5 and 7 hamster died after week 2 p.i. and week 4 p.i., respectively.

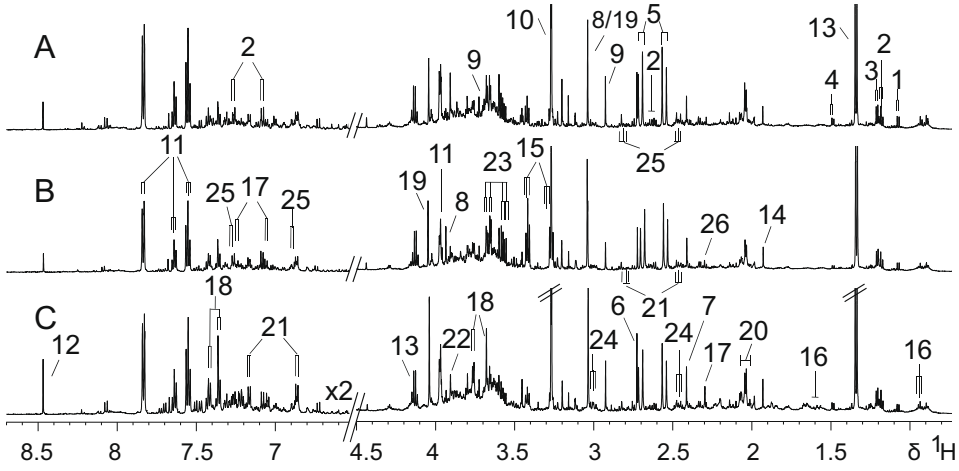

Fig. 1. Typical 600 MHz ^{1}H nuclear magnetic resonance spectra of urine obtained from hamsters pre-infection (A) at week 2 p.i. with *Schistosoma japonicum* and *Necator americanus* co-infection (B) and at week 4 p.i. (C). The spectra in the aromatic region (δ 6.5–8.7) were magnified twice compared with the region of δ 0.8–4.5. Key: 1: dihydrothymine; 2: 4-ethylphenol; 3: D-3-hydroxybutyrate; 4: alanine; 5: citrate; 6: dimethylamine; 7: succinate; 8: creatine; 9: dimethylglycine; 10: trimethylamine-*N*-oxide; 11: hippurate; 12: formate; 13: lactate; 14: acetate; 15: taurine; 16: butyrate; 17: 4-cresol glucuronide; 18: phenylacetylglycine; 19: creatinine; 20: *N*-acetylglycoproteins; 21: 4-hydroxyphenylpropionic acid; 22: betaine; 23: glycerol; 24: 2-oxoglutarate; 25: 3-hydroxyphenylpropionic acid; 26: acetone.

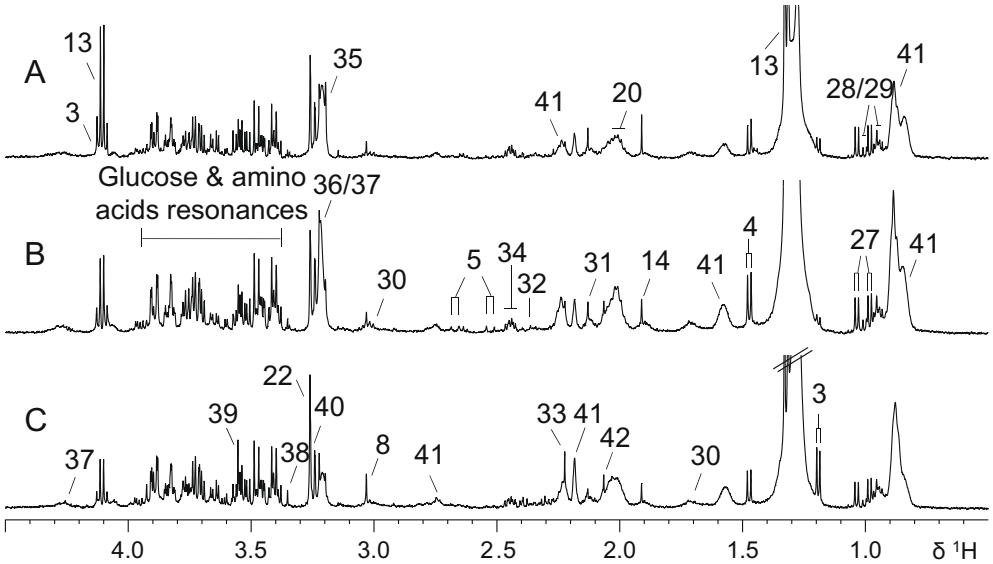

Fig. 2. Typical 500 MHz ^{1}H Carr–Purcell–Meiboom–Gill nuclear magnetic resonance spectra of serum obtained from hamsters pre-infection (A), at week 2 p.i. with *Schistosoma japonicum* and *Necator americanus* co-infection (B) and at week 4 p.i. (C). Key: 3: D-3-hydroxybutyrate; 4: alanine; 5: citrate; 8: creatine; 13: lactate; 14: acetate; 20: *N*-acetylglycoproteins 22: betaine; 27: valine; 28: leucine; 29: isoleucine; 30: lysine; 31: methionine; 32: pyruvate; 33: acetoacetate; 34: glutamate; 35: choline; 36: phosphorylcholine; 37: glyceryl phosphorylcholine; 38: *scyllo*-inositol; 39: glycine; 40: glucose; 41: lipoprotein lipids; 42: *O*-acetylglycoproteins.

parisons between infected and control groups were subsequently performed for all of the sampling time points using an O-PLS-DA strategy. One PLS component and one orthogonal component were calculated for all of the models using NMR spectral data as the X matrix and classification information as the dummy Y matrix. Permutation tests were applied to validate the models and the results suggested that models constructed from urine spectral data at weeks 4 and 5 p.i. were valid (data not shown). However, a stronger model was derived for spectra obtained at week 5 p.i. ($R^2 = 0.50$, $Q^2 = 0.84$) than week 4 p.i. ($R^2 = 0.38$, $Q^2 = 0.77$).

O-PLS-DA cross-validated score plots illustrated a clear separation between urine spectra obtained from control and co-infected hamsters at weeks 4 and 5 p.i. (Fig. 3A and C) with a greater variation along the orthogonal axes for the infected individuals compared with control hamsters, probably due to variation among individual hamsters in response to the co-infection. The corresponding co-efficient plots (Fig. 3B and D) displayed important metabolites contributing to the differentiation. Here, correlation coefficients higher than 0.67 were regarded as significant in the discrimination based on a 95% confidence limit ($n_1 = 10$, $n_2 = 8$). The urinary metabolic response of hamsters co-infected with *S. japonicum* and *N. americanus* at week 4 p.i. was characterised by lower concentrations of tricarboxylic acid (TCA) cycle intermediates such as citrate, succinate and a series of gut microbiotal-related metabolites, including hippurate and 3-HPPA. These alterations are also associated with relatively higher concentrations of creatine in the urine of the co-infected hamsters. As the co-infection progressed to week 5 p.i., additional variations in metabolite composition were noted; decreased levels of betaine and TMAO with increased levels of 4-cresol glucuronide and PAG were observed in urine from infected hamsters. These changes are summarised in Table 2.

For the purpose of comparison between single versus co-infection, the variation in urinary metabolite profiles of hamster associated with a single infection of *S. japonicum* or *N. americanus* was extracted from our previously published work (Wang et al., 2006, 2009) and summarised in Table 2. Increased levels of urinary 4-cresol glucuronide and PAG, and decreased levels of urinary hippurate were common for both types of single infection, as well as the *N. americanus* and *S. japonicum* co-infected animals. Elevated levels of 2-aminoadipate and depleted levels of 2-ketoisocaproate, DMA, 4-hydroxy-3-methy-phenylpropionic acid and 4-HPPA were associated only with a *N. americanus* infection, whereas elevated levels of pyruvate and trimethylamine (TMA) were only associated with a *S. japonicum* infection. Variations of 4-ethylphenol, alanine, *N*-acetylglycoprotein and 3-HPPA were only seen in the co-infected hamsters.

3.4. Metabolic profiling via ^{1}H NMR spectroscopy of serum

The same analytical approach was applied to the CPMG ^{1}H NMR spectral data of serum. Permutation tests suggested that the models constructed from spectra collected at the three time points, day 1 and weeks 4 and 5 p.i., were predictive. The differences between sera obtained from non-infected control and co-infected hamsters increased from week 4 p.i. ($R^2 = 0.22$, $Q^2 = 0.68$) to week 5 p.i. ($R^2 = 0.41$, $Q^2 = 0.87$), reflected by the higher Q^2 value generated from the later time-point model. The corresponding coefficients plots shown in Fig. 4 illustrated the increase in concentrations of lipoproteins and depleted levels of amino acids and membrane-related metabolites, such as choline and phosphorylcholine/GPC, in the infected hamsters. It was also found that the levels of D-3-HB were highly correlated with the infection at week 4 p.i., and that the levels of citrate and glucose decreased towards the end of the experiment (lower levels at 5 weeks p.i. compared with 4 weeks p.i.). The changes in metabolites in hamster sera, as a response to co-infection, are summarised in Table 3.

4. Discussion

Epidemiological studies have shown that polyparasitism is the norm rather than the exception, particularly in developing countries (Petney and Andrews, 1998; McKenzie, 2005). However, metabolic alterations in a host due to multiple parasitic infections remain largely unexplored. Here, we characterised the metabolic fingerprint of a *N. americanus–S. japonicum* co-infection in a hamster model, as a first step towards identifying interactions between multiple parasites harboured simultaneously in a single host. To our knowledge, this is the first application of metabonomics to the investigation of the metabolic response of a rodent host to co-infection with two helminth species.

An important finding of our investigation is that, upon dissection, *N. americanus* and *S. japonicum* worm burdens in co-infected hamsters did not differ significantly from single infection models (Table 1), i.e. there was no suggestion of enhancement or inhibition of worm burden as a response to co-infection. Recently, Graham (2008) discussed two processes governing the ecology of co-infection of helminths with micro-parasites: (i) when two parasites compete for the same resource for survival, reduced micro-parasite density would occur and (ii) when a helminth infection suppresses

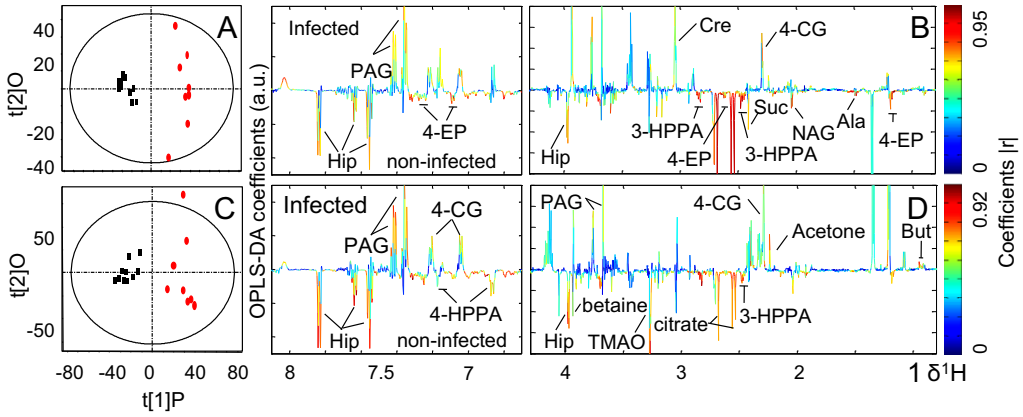

Fig. 3. Orthogonal projection to latent structure discriminant analysis scores (A, C) and co-efficient (B, D) plots generated from pair-wise comparison between urine spectra obtained from non-infected (black boxes) and from *Schistosoma japonicum* and *Necator americanus* co-infected (red dots) hamsters at week 4 p.i. (A) and week 5 p.i. (C). Key: 4-CG: 4-cresol glucuronide; 4-EP: 4-ethylphenol; 3-HPPA: 3-hydroxyphenylpropionic acid; 4-HPPA: 4-hydroxyphenylpropionic acid; Ala: alanine; But: butyrate; Cre: creatine; Hip: hippurate; NAG: *N*-acetylglycoprotein; PAG: phenylacetylglycine; Suc: succinate; TMAO: trimethylamine-*N*-oxide.

Table 2
Alterations in urinary metabolites of hamsters after co-infection of *Schistosoma japonicum* and *Necator americanus*.

Metabolites	Chemical shift (ppm)	Co-infection_urine		*S. japonicum*	*N. americanus*
		4 weeks p.i. $R^2 = 0.38$, $Q^2 = 0.77$	5 weeks p.i. $R^2 = 0.50$, $Q^2 = 0.84$	5 weeks p.i. (Wang et al., 2006)	5 weeks p.i. (Wang et al., 2009)
2-Ketoisocaproate	0.92(d)				↓
Butyrate	0.94(t)	0.55(↑)	0.83(↑)[a]		↓
4-Ethylphenol	1.18(t), 2.61(m)	0.87(↓)[a]	0.85(↓)[a]		
Alanine	1.48(d)	0.90(↓)[a]	0.37(↓)		
N-Acetylglycoprotein	2.03(b)	0.85(↓)[a]	0.56(↓)		
2-Aminoadipate	2.20(m), 1.87(m), 1.65(m)				↑
Acetone	2.23(s)	0.34(↑)	0.75(↑)[a]		
4-Hydroxy-3-methy-phenylpropionate acid	2.46(t), 2.82(t), 3.87(s)				↓
Creatine	3.03(s)	0.78(↑)[a]	0.35(↑)		↑
Betaine	3.9(s)	0.41(↓)	0.68(↓)[a]		
Pyruvate	2.34(s)			↑	
Succinate	2.41(s)	0.77(↓)[a]	0.29(↓)	↓	
Citrate	2.54(d)	0.90(↓)[a]	0.82(↓)[a]	↓	
3-HPPA	2.48(t), 2.84(t)	0.91(↓)[a]	0.89(↓)[a]		
4-HPPA	2.45(t), 2.81(t), 6.85(d)	0.84(↓)[a]	0.78(↓)[a]		↓
DMA	2.72(s)	0.57(↓)	0.46(↓)		↓
TMA	2.88(s)			↑	
TMAO	3.27(s)	0.42(↓)	0.86(↓)[a]		
PAG	3.68(s), 3.75(d)	0.62(↑)	0.77(↑)[a]	↑	↑
4-Cresol glucuronide	2.29(s)	0.74(↑)[a]	0.72(↑)[a]	↑	↑
Hippurate	3.97(d)	0.76(↓)[a]	0.88(↓)[a]	↓	↓

3-HPPA: 3-hydroxyphenylpropionic acid; 4-HPPA: 4-hydroxyphenylpropionic acid; DMA: dimethylamine; TMA: trimethylamine; TMAO: trimethylamine-*N*-oxide; PAG: phenylacetylglycine.

[a] Significant changes at the 95% confidence limit; ↑: increase in concentration; ↓: decrease in concentration; s: singlet; d: doublets; t: triples; m: multiples; b: broad peak.

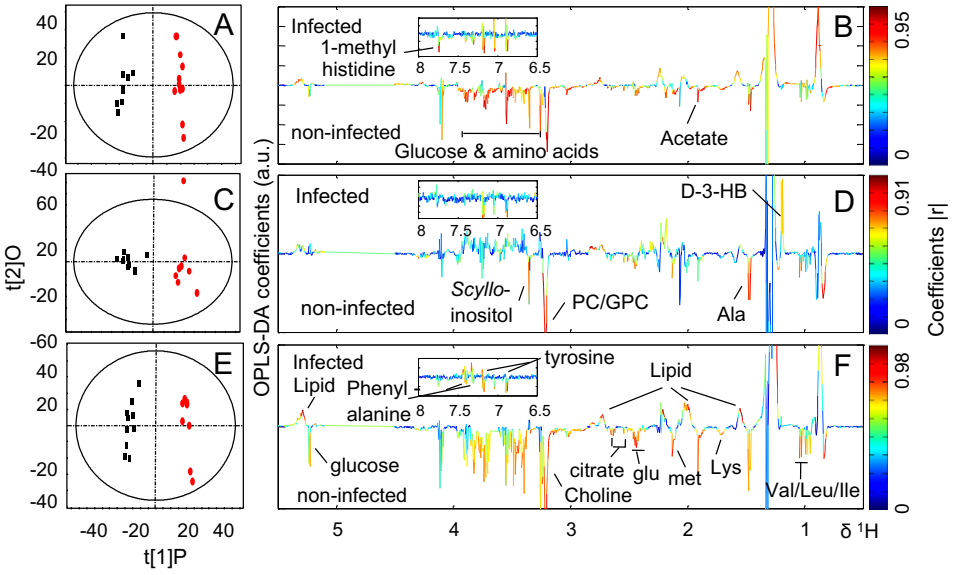

Fig. 4. Orthogonal projection to latent structure discriminant analysis scores (A, C, E) and co-efficient (B, D, F) plots generated from pair-wise comparison between serum Carr–Purcell–Meiboom–Gill spectra obtained from non-infected (black boxes) and *Schistosoma japonicum* and *Necator americanus* co-infected (red dots) hamsters at day 1 p.i. (A), week 4 p.i. (C) and week 5 p.i. (E). Key: D-3-HB: D-3-hydroxybutyrate; Ala: alanine; Glu: glutamate; PC: phosphorylcholine; GPC: glyceryl phosphorylcholine; Ile: isoleucine; Leu: leucine; Lys: lysine; Met: methionine; Val: valine.

the immune response of a host, increased micro-parasite density would occur (Graham, 2008). The situation for co-infection with multiple helminths is undoubtedly more complex. Previously, a concurrent *Schistosoma* infection has been found to augment the severity of malaria and hookworm disease (Naus et al., 2003; Raso et al., 2004). In contrast, in the case of *Schistosoma* and *T. muris*, a reduction in *T. muris* burden was observed (Curry et al., 1995). In the present investigation, since both helminth species are blood-feeding parasites and thus compete for the same resource, inhibition of growth for either or both might be expected since the co-infection was executed simultaneously. It would be of interest to evaluate the impact of a super-infection in a host already harbouring an infection with a single parasite species, i.e. investigate co-infection models whereby the introduction of one parasite is temporarily delayed.

It is interesting to note that metabolic profiles of sera of co-infected hamsters differed markedly from matched controls from day 1 p.i., but appeared recover before deviating from the matched

Table 3
Variations in serum metabolites of hamsters after co-infection of *Schistosoma japonicum* and *Necator americanus*.

Metabolites	Chemical shift (ppm)	Co-infection_serum			*N. americanus*
		1 day p.i. $R^2 = 0.43$, $Q^2 = 0.87$	4 weeks p.i. $R^2 = 0.22$, $Q^2 = 0.68$	5 weeks p.i. $R^2 = 0.41$, $Q^2 = 0.87$	5 weeks p.i. (Wang et al., 2009)
Lipid	0.88, 1.25, 1.55, 2.03, 2.23, 2.75, 5.30	0.92(↑)[a]	0.86(↑)[a]	0.97(↑)[a]	↑
Leucine	0.95(d)	0.61(↓)	0.46(↓)	0.78(↓)[a]	
Isoleucine	1.01(d)	0.53(↓)	0.78(↓)[a]	0.76(↓)[a]	↓
Valine	1.03(d)	0.72(↓)[a]	0.78(↓)[a]	0.84(↓)[a]	↓
D-3-HB	1.2(d)	0.23(↓)	0.82(↑)[a]	0.20(↑)	
Lysine	1.45(m), 3.01(m)	0.84(↓)[a]	0.53(↓)	0.79(↓)[a]	
Alanine	1.48(d)	0.87(↓)[a]	0.84(↓)[a]	0.83(↓)[a]	
Acetate	1.91(s)	0.85(↓)[a]	0.55(↓)	0.77(↓)[a]	↓
Methionine	2.13(s), 2.62(t)	0.87(↓)[a]	0.62(↓)	0.84(↓)[a]	
Glutamate	2.13(m), 2.45(m)	0.92(↓)[a]	0.76(↓)[a]	0.86(↓)[a]	
Citrate	2.52(d), 2.66(d)	0.85(↓)[a]	0.72(↓)[a]	0.90(↓)[a]	
Creatine	3.03(s)	0.80(↓)[a]	0.32(↑)	0.42(↓)	
Choline	3.2(s)	0.87(↓)[a]	0.80(↓)[a]	0.90(↓)[a]	
GPC/phosphorylcholine	3.22(s)	0.33(↓)	0.83(↓)[a]	0.88(↓)[a]	↓
Glucose	3.24(dd)	0.72(↓)[a]	0.08(↑)	0.77(↓)[a]	↓
TMAO	3.26(s)	0.82(↓)[a]	0.11(↑)	0.74(↓)[a]	
Scyllo-inositol	3.35(s)	0.85(↓)[a]	0.75(↓)[a]	0.14(↑)	
Glycine	3.55(s)	0.87(↓)[a]	0.33(↑)	0.63(↓)	↑
Tyrosine	6.8(d), 7.17(d)	0.89(↓)[a]	0.78(↓)[a]	0.84(↓)[a]	
Phenylalanine	7.32(m), 7.43(m)	0.83(↓)[a]	0.22(↓)	0.93(↓)[a]	
1-Methyl-histidine	7.04(s), 7.75(s)	0.91(↓)[a]	0.58(↓)	0.56(↓)	

D-3-HB: D-3-hydroxybutyrate; GPC: glyceryl phosphorylcholine; TMAO: trimethylamine-*N*-oxide.
[a] Significant changes at the 95% confidence limit; ↑: increase in concentration; ↓: decrease in concentration; s: singlet; d: doublets; dd, doublet of doublets, t: triples; m: multiples.

controls again at the later stage of the infection. A similar observation was made in mice infected with *T. brucei brucei* (Wang et al., 2008). The initial rapid metabolic response phase is likely attributable to the host immune response (Newsholme et al., 2003).

In order to reduce the number of animals included in this experiment, since the metabolic perturbations in laboratory host–parasite models have been shown to be robust and reproducible (Garcia-Perez et al., 2008; Li et al., 2009), and in line with the 3R rules (replace, reduce and refine), single infection groups were not included in the analysis, since they are already described in the literature (Wang et al., 2006, 2009). Therefore it is not appropriate to make any inference regarding comparative severity of the observed metabolic changes; rather we concentrate here on the effect of co-infection on the qualitative disturbance of metabolic profiles. In the current investigation, we noted depletion of amino acids in the sera of co-infected hamsters. This observation was also made in the individually-infected animal host with *S. japonicum* or *N. americanus* (Li et al., 2009; Wang et al., 2009). It is well documented that schistosomiasis causes liver injury, resulting in disturbance of amino acid metabolism. This manifests itself in the accumulation of amino acids in the liver and depletion of those in plasma (Wang et al., 2004). The process of depletion of branched-chain amino acids (BCAAs) could serve as an energy source, as previously observed in *S. mansoni*-infected mice and *N. americanus*-infected hamsters (Wang et al., 2004, 2009), since these amino acids are capable of producing keto-acids, such as 2-ketoisovalerate and 2-ketoisocaproate via aminotransferases, which can be used as an alternative energy source (Hutson and Hall, 1993).

Another prominent finding of the present study was the marked reduction in levels of glucose and TCA intermediates, such as citrate and succinate, in the co-infected hamsters. This observation is consistent with rodents singly infected with either *S. mansoni* or *S. japonicum* (Wang et al., 2004, 2006). Our current results suggest that stimulated glycolysis and depression of the TCA cycle were associated with hosts co-infected with *S. japonicum* and *N. americanus*, as well as with hosts infected with *Schistosoma* spp. alone. In support of this finding, several enzyme activities related to the carbohydrate metabolism (such as increased pyruvate kinase and phosphofructokinase, and decreased citrate synthase and glycogen phosphorylase) were found in the hosts with a *Schistosoma* spp. infection (Ahmed and Gad, 1995). Hypoglycaemia was reported in the *Nippostrongylus brasiliensis*-infected rat and the *N. americanus*-infected hamster (Wang et al., 2009) due to marked catabolism and reduction of food intake after the infection (Ovington, 1986). This leads to clinical anaemia of infected hosts, which is known to be further enhanced by co-infection (Hotez et al., 2004; Ezeamama et al., 2005).

Increased levels of lipids were observed in the sera of co-infected hamsters at week 5 p.i., but not at week 4 p.i. Previous investigations have shown that adult schistosomes are capable of taking up phospholipids and triacylglycerols from the host to form lipid tegument (Allan et al., 1987; Brouwers et al., 1997), resulting in decreased lipids in host serum (Liu et al., 2007). In contrast to a *Schistosoma* spp. infection, profound twofold hyperlipidemia and fourfold hypertriglyceridemia associated with the down-regulation of plasma lecithin cholesterol acyl transferase activity were observed in the *Ancylostoma ceylanicum* (another hookworm species)-infected hamster (Ovington, 1987). The hypertriglyceridemia associated with hookworm infection was reported to be caused by the decreased lipolytic activity or defective catabolic process (Mukerjee et al., 1988, 1990). The hyperlipidemia was further characterised by an increase in very low density lipoproteins (VLDL) and low density lipoproteins (LDL) with a concomitant decline in high density lipoproteins (HDL) during experimental ancylostomiasis, which coincides with our observation for the co-infected hamsters (Table 3). Our current observation of lipid levels that remained unchanged at week 4 p.i., but showed increased levels at the final observation time point (i.e. week 5 p.i.), is likely due to the balance between the two infections, i.e. increase in lipids associated with hookworm infection and decrease in lipids caused by *Schistosoma* spp. infection.

A reduction in the concentrations of membrane metabolites such as phosphorylcholine and GPC was a common effect for both co-infected hamsters and for rodent hosts infected with *Schisto-*

soma spp. or *N. americanus* singly. A previous investigation of *A. ceylanicum*-infected hamsters also found a significant decrease in the phospholipid/cholesterol ratio and plasma membrane protein, as direct results of reduced activities of nucleotidase, gamma-glutamyl transpeptidase, Na^+/K^+-ATPase, Ca^{2+}-ATPase and Mg^{2+}-ATPase in infected animals (Srivastava, 1994).

In the present investigation, we observed alterations in a series of gut microbiotal-related metabolites in the co-infected hamsters, such as the reduced concentrations of hippurate, TMAO, 3-HPPA and elevated levels of 4-cresol glucuronide and PAG. It was known that PAG and 4-cresol glucuronide are involved in metabolism of the aromatic amino acids, and that phenylalanine and tyrosine are initially converted to phenylacetic acid and hydroxylphenylacetate, respectively, by intestinal bacteria. Hydroxylphenylacetate is further decarboxylated to 4-cresol by enterobacteria under anaerobic conditions. Once absorbed, phenylacetic acid and 4-cresol are conjugated with glycine and glucuronide, respectively, via phase II of detoxication in the liver, producing PAG and 4-cresol glucuronide. Variations in the concentrations of hippurate can also occur following colonisation and subsequent redistribution of gut microbiota (Nicholls et al., 2003). Among these altered gut-microbiotal-related metabolites, the decreased level of hippurate and increased levels of 4-cresol glucuronide and PAG appeared to be common to all helminth infections studied to date (Wang et al., 2004, 2006, 2009; Saric et al., 2008, 2009). Further investigation of alterations of microbiota associated with these infections is clearly necessary for understanding the relationship between microbiotal-mammalian metabolites in the urine signature.

In conclusion, we have demonstrated that metabolic profiles in hamsters co-infected with two parasites are the consequence of combined metabolic effects that are also consistent with responses to the respective single infections. Future work should be focused on the impact of super-infection in a host already harbouring a patent infection with one parasite in terms of worm burden and corresponding alterations of metabolic profiles. A deeper understanding of parasite-induced disturbance of gut microbiota could provide new insight into mechanisms of three-way interactions of host-parasites-microbiota. Furthermore, an enhanced understanding of metabolic alterations induced by parasitic infection could provide vital information for targeted drug discovery for a more efficacious treatment and possible prevention of parasitic diseases.

Acknowledgements

The authors thank Dr. Zhu Hang (Wuhan Institute of Physics and Mathematics, Chinese Academy of Sciences, People's Republic of China) for providing Matlab scripts for the colour-coded coefficients plot. Financial support from Chinese Academy of Sciences (the 100T program for H.T.; the Knowledge Innovation Program for Y.W. with Grant KJXC2-YW-W11) and NSFC (National Award for the Outstanding Young Scientists for H.T.) are acknowledged. J.U. is grateful to the Swiss National Science Foundation (Grant Nos. PPOOB-102883, PPOOB-119129).

References

Ahmed, S.A., Gad, M.Z., 1995. Effect of schistosomal infection and its treatment on some key enzymes of glucose metabolism in mice livers. Arzneimittelforschung 45, 1324–1328.

Allan, D., Payares, G., Evans, W.H., 1987. The phospholipid and fatty acid composition of *Schistosoma mansoni* and of its purified tegumental membranes. Mol. Biochem. Parasitol. 23, 123–128.

Behnke, J.M., Bajer, A., Sinski, E., Wakelin, D., 2001. Interactions involving intestinal nematodes of rodents: experimental and field studies. Parasitology 122 (Suppl.), S39–S49.

Bollard, M.E., Stanley, E.G., Lindon, J.C., Nicholson, J.K., Holmes, E., 2005. NMR-based metabonomic approaches for evaluating physiological influences on biofluid composition. NMR Biomed. 18, 143–162.

Brindle, J.T., Antti, H., Holmes, E., Tranter, G., Nicholson, J.K., Bethell, H.W., Clarke, S., Schofield, P.M., McKilligin, E., Mosedale, D.E., Grainger, D.J., 2002. Rapid and noninvasive diagnosis of the presence and severity of coronary heart disease using ^{1}H-NMR-based metabonomics. Nat. Med. 8, 1439–1444.

Brito, L.L., Barreto, M.L., Silva Rde, C., Assis, A.M., Reis, M.G., Parraga, I.M., Blanton, R.E., 2006. Moderate- and low-intensity co-infections by intestinal helminths and *Schistosoma mansoni*, dietary iron intake, and anemia in Brazilian children. Am. J. Trop. Med. Hyg. 75, 939–944.

Brouwers, J.F., Smeenk, I.M., van Golde, L.M., Tielens, A.G., 1997. The incorporation, modification and turnover of fatty acids in adult *Schistosoma mansoni*. Mol. Biochem. Parasitol. 88, 175–185.

Cloarec, O., Dumas, M.E., Trygg, J., Craig, A., Barton, R.H., Lindon, J.C., Nicholson, J.K., Holmes, E., 2005. Evaluation of the orthogonal projection on latent structure model limitations caused by chemical shift variability and improved visualization of biomarker changes in ^{1}H NMR spectroscopic metabonomic studies. Anal. Chem. 77, 517–526.

Correa-Oliveira, R., Golgher, D.B., Oliveira, G.C., Carvalho, O.S., Massara, C.L., Caldas, I.R., Colley, D.G., Gazzinelli, G., 2002. Infection with *Schistosoma mansoni* correlates with altered immune responses to *Ascaris lumbricoides* and hookworm. Acta Trop. 83, 123–132.

Curry, A.J., Else, K.J., Jones, F., Bancroft, A., Grencis, R.K., Dunne, D.W., 1995. Evidence that cytokine-mediated immune interactions induced by *Schistosoma mansoni* alter disease outcome in mice concurrently infected with *Trichuris muris*. J. Exp. Med. 181, 769–774.

Ezeamama, A.E., Friedman, J.F., Olveda, R.M., Acosta, L.P., Kurtis, J.D., Mor, V., McGarvey, S.T., 2005. Functional significance of low-intensity polyparasite helminth infections in anemia. J. Infect. Dis. 192, 2160–2170.

Fan, W.M.T., 1996. Metabolite profiling by one- and two-dimensional NMR analysis of complex mixtures. Prog. Nucl. Magn. Reson. Spectrosc. 28, 161–219.

Fenton, A., Lamb, T., Graham, A.L., 2008. Optimality analysis of Th1/Th2 immune responses during microparasite–macroparasite co-infection, with epidemiological feedbacks. Parasitology 135, 841–853.

Fleming, F.M., Brooker, S., Geiger, S.M., Caldas, I.R., Correa-Oliveira, R., Hotez, P.J., Bethony, J.M., 2006. Synergistic associations between hookworm and other helminth species in a rural community in Brazil. Trop. Med. Int. Health 11, 56–64.

Garcia-Perez, I., Whitfield, P., Bartlett, A., Angulo, S., Legido-Quigley, C., Hanna-Brown, M., Barbas, C., 2008. Metabolic fingerprinting of *Schistosoma mansoni* infection in mice urine with capillary electrophoresis. Electrophoresis 29, 3201–3206.

Graham, A.L., 2008. Ecological rules governing helminth-microparasite coinfection. Proc. Natl. Acad. Sci. USA 105, 566–570.

Hotez, P.J., Brooker, S., Bethony, J.M., Bottazzi, M.E., Loukas, A., Xiao, S., 2004. Hookworm infection. N. Engl. J. Med. 351, 799–807.

Hutson, S.M., Hall, T.R., 1993. Identification of the mitochondrial branched chain aminotransferase as a branched chain alpha-keto acid transport protein. J. Biol. Chem. 268, 3084–3091.

Keiser, J., N'Goran, E.K., Singer, B.H., Lengeler, C., Tanner, M., Utzinger, J., 2002. Association between *Schistosoma mansoni* and hookworm infections among schoolchildren in Côte d'Ivoire. Acta Trop. 84, 31–41.

Keusch, G.T., Migasena, P., 1982. Biological implications of polyparasitism. Rev. Infect. Dis. 4, 880–882.

Lamb, T.J., Graham, A.L., Le Goff, L., Allen, J.E., 2005. Co-infected C57BL/6 mice mount appropriately polarized and compartmentalized cytokine responses to *Litomosoides sigmodontis* and *Leishmania major* but disease progression is altered. Parasite Immunol. 27, 317–324.

Li, J.V., Wang, Y.L., Saric, J., Nicholson, J.K., Dirnhofer, S., Singer, B.H., Tanner, M., Wittlin, S., Holmes, E., Utzinger, J., 2008. Global metabolic responses of NMRI mice to an experimental *Plasmodium berghei* infection. J. Proteome Res. 7, 3948–3956.

Li, J.V., Holmes, E., Saric, J., Keiser, J., Dirnhofer, S., Utzinger, J., Wang, Y.L., 2009. Metabolic profiling of a *Schistosoma mansoni* infection in mouse tissues using magic angle spinning-nuclear magnetic resonance spectroscopy. Int. J. Parasitol. 39, 547–558.

Liu, F., Hu, W., Cui, S.J., Chi, M., Fang, C.Y., Wang, Z.Q., Yang, P.Y., Han, Z.G., 2007. Insight into the host–parasite interplay by proteomic study of host proteins copurified with the human parasite, *Schistosoma japonicum*. Proteomics 7, 450–462.

McKenzie, F.E., 2005. Polyparasitism. Int. J. Epidemiol. 34, 221–222.

Mukerjee, S., Tekwani, B.L., Tripathi, L.M., Maitra, S.C., Visen, P.K., Katiyar, J.C., Ghatak, S., 1988. Biochemical and histopathological alterations in golden hamster during infection with *Ancylostoma ceylanicum*. Exp. Mol. Pathol. 49, 50–61.

Mukerjee, S., Chander, R., Tekwani, B.L., Gupta, S., Katiyar, J.C., Shukla, O.P., Kapoor, N.K., 1990. Molecular basis of hyperlipidemia in golden hamsters during experimental infection with *Ancylostoma ceylanicum* (Nematoda:Strongylidae). Int. J. Parasitol. 20, 217–223.

Naus, C.W., Jones, F.M., Satti, M.Z., Joseph, S., Riley, E.M., Kimani, G., Mwatha, J.K., Kariuki, C.H., Ouma, J.H., Kabatereine, N.B., Vennervald, B.J., Dunne, D.W., 2003. Serological responses among individuals in areas where both schistosomiasis and malaria are endemic: cross-reactivity between *Schistosoma mansoni* and *Plasmodium falciparum*. J. Infect. Dis. 187, 1272–1282.

Newsholme, P., Lima, M.M., Procopio, J., Pithon-Curi, T.C., Doi, S.Q., Bazotte, R.B., Curi, R., 2003. Glutamine and glutamate as vital etabolites. Braz. J. Med. Biol. Res. 36, 153–163.

Nicholls, A.W., Mortishire-Smith, R.J., Nicholson, J.K., 2003. NMR spectroscopic-based metabonomic studies of urinary metabolite variation in acclimatizing germ-free rats. Chem. Res. Toxicol. 16, 1395–1404.

Nicholson, J.K., Foxall, P.J., Spraul, M., Farrant, R.D., Lindon, J.C., 1995. 750 MHz ^{1}H and ^{1}H–^{13}C NMR spectroscopy of human blood plasma. Anal. Chem. 67, 793–811.

Ovington, K.S., 1986. Physiological responses of rats to primary infection with *Nippostrongylus brasiliensis*. J. Helminthol. 60, 307–312.

Ovington, K.S., 1987. *Nippostrongylus brasiliensis*: physiological and metabolic responses of rats to primary infection. Exp. Parasitol. 63, 10–20.

Petney, T.N., Andrews, R.H., 1998. Multiparasite communities in animals and humans: frequency, structure and pathogenic significance. Int. J. Parasitol. 28, 377–393.

Pullan, R.L., Bethony, J.M., Geiger, S.M., Cundill, B., Correa-Oliveira, R., Quinnell, R.J., Brooker, S., 2008. Human helminth co-infection: analysis of spatial patterns and risk factors in a Brazilian community. PLoS Negl. Trop. Dis. 2, e352.

Raso, G., Luginbuhl, A., Adjoua, C.A., Tian-Bi, N.T., Silue, K.D., Matthys, B., Vounatsou, P., Wang, Y.L., Dumas, M.E., Holmes, E., Singer, B.H., Tanner, M., N'Goran, E.K., Utzinger, J., 2004. Multiple parasite infections and their relationship to self-reported morbidity in a community of rural Côte d'Ivoire. Int. J. Epidemiol. 33, 1092–1102.

Raso, G., Vounatsou, P., Gosoniu, L., Tanner, M., N'Goran, E.K., Utzinger, J., 2006. Risk factors and spatial patterns of hookworm infection among schoolchildren in a rural area of western Côte d'Ivoire. Int. J. Parasitol. 36, 201–210.

Saric, J., Li, J.V., Wang, Y.L., Keiser, J., Bundy, J.G., Holmes, E., Utzinger, J., 2008. Metabolic profiling of an *Echinostoma caproni* infection in the mouse for biomarker discovery. PLoS Negl. Trop. Dis. 2, e254.

Saric, J., Li, J.V., Wang, Y.L., Keiser, J., Veselkov, K., Dirnhofer, S., Yap, I.K., Nicholson, J.K., Holmes, E., Utzinger, J., 2009. Panorganismal metabolic response modeling of an experimental *Echinostoma caproni* infection in the mouse. J. Proteome Res. 8, 3899–3911.

Slupsky, C.M., Rankin, K.N., Wagner, J., Fu, H., Chang, D., Weljie, A.M., Saude, E.J., Lix, B., Adamko, D.J., Shah, S., Greiner, R., Sykes, B.D., Marrie, T.J., 2007. Investigations of the effects of gender, diurnal variation, and age in human urinary metabolomic profiles. Anal. Chem. 79, 6995–7004.

Sreekumar, A., Poisson, L.M., Rajendiran, T.M., Khan, A.P., Cao, Q., Yu, J., Laxman, B., Mehra, R., Lonigro, R.J., Li, Y., Nyati, M.K., Ahsan, A., Kalyana-Sundaram, S., Han, B., Cao, X., Byun, J., Omenn, G.S., Ghosh, D., Pennathur, S., Alexander, D.C., Berger, A., Shuster, J.R., Wei, J.T., Varambally, S., Beecher, C., Chinnaiyan, A.M., 2009. Metabolomic profiles delineate potential role for sarcosine in prostate cancer progression. Nature 457, 910–914.

Srivastava, S.C., 1994. Liver plasma membrane-bound enzymes and lipids in golden hamsters infected with *Ancylostoma ceylanicum*. Int. J. Parasitol. 24, 249–251.

Steinmann, P., Du, Z.W., Wang, L.B., Wang, X.Z., Jiang, J.Y., Li, L.H., Marti, H., Zhou, X.N., Utzinger, J., 2008. Extensive multiparasitism in a village of Yunnan province, People's Republic of China, revealed by a suite of diagnostic methods. Am. J. Trop. Med. Hyg. 78, 760–769.

Timothy, L.M., Coulson, P.S., Behnke, J.M., Wilson, R.A., 1992. Cross-reactivity between *Necator americanus* and *Schistosoma mansoni* in mice. Int. J. Parasitol. 22, 1143–1149.

Trygg, J., Wold, S., 2002. Orthogonal projections to latent structures (O-PLS). J. Chemom. 16, 119–128.

Trygg, J., Holmes, E., Lundstedt, T., 2007. Chemometrics in metabonomics. J. Proteome Res. 6, 469–479.

Vandenberg, R.A., Hoefsloot, H.C.J., Westerhuis, J.A., Smilde, A.K., Vanderwerf, M.J., 2006. Centering, scaling, and transformations: improving the biological information content of metabolomics data. BMC Genomics 7, 142–156.

Wang, Y.L., Holmes, E., Nicholson, J.K., Cloarec, O., Chollet, J., Tanner, M., Singer, B.H., Utzinger, J., 2004. Metabonomic investigations in mice infected with *Schistosoma mansoni*: an approach for biomarker identification. Proc. Natl. Acad. Sci. USA 101, 12676–12681.

Wang, Y.L., Utzinger, J., Xiao, S.H., Xue, J., Nicholson, J.K., Tanner, M., Singer, B.H., Holmes, E., 2006. System level metabolic effects of a *Schistosoma japonicum* infection in the Syrian hamster. Mol. Biochem. Parasitol. 146, 1–9.

Wang, Y.L., Utzinger, J., Saric, J., Li, J.V., Burckhardt, J., Dirnhofer, S., Nicholson, J.K., Singer, B.H., Brun, R., Holmes, E., 2008. Global metabolic responses of mice to *Trypanosoma brucei brucei* infection. Proc. Natl. Acad. Sci. USA 105, 6127–6132.

Wang, Y.L., Xiao, S.H., Xue, J., Singer, B.H., Utzinger, J., Holmes, E., 2009. Systems metabolic effects of a *Necator americanus* infection in Syrian hamster. J. Proteome Res. 8, 5442–5450.

Westerhuis, J.A., Hoefsloot, J.C., Smit, S., Vis, D.J., Smilde, A.K., van Velzen, E.J., van Duijnhoven, J.P.M., van Dorsten, F.A., 2008. Assessment of PLSDA cross validation. Metabolomics 4, 81–89.

Xiao, C., Hao, F., Qin, X., Wang, Y., Tang, H., 2009. An optimized buffer system for NMR-based urinary metabonomics with effective pH control, chemical shift consistency and dilution minimization. Analyst 134, 916–925.

Xue, J., Liu, S., Qiang, H.Q., Ren, H.N., Li, T.H., Xue, H.C., Hotez, P.J., Xiao, S.H., 2003. *Necator americanus*: maintenance through one hundred generations in golden hamsters (*Mesocricetus auratus*). I. Host sex-associated differences in hookworm burden and fecundity. Exp. Parasitol. 104, 62–66.

Yoshida, A., Maruyama, H., Yabu, Y., Amano, T., Kobayakawa, T., Ohta, N., 1999. Immune response against protozoal and nematodal infection in mice with underlying *Schistosoma mansoni* infection. Parasitol. Int. 48, 73–79.

Yu, S.H., Xu, L.Q., Jiang, Z.X., Xu, S.H., Han, J.J., Zhu, Y.G., Chang, J., Lin, J.X., Xu, F.N., 1994. Nationwide survey of human parasite in China. Southeast Asian J. Trop. Med. Public Health 25, 4–10.